

A closer look at the training dynamics of knowledge distillation

Roy Miles
Imperial College London
r.miles18@imperial.ac.uk

Krystian Mikolajczyk
Imperial College London
k.mikolajczyk@imperial.ac.uk

Abstract

In this paper we revisit the efficacy of knowledge distillation as a function matching and metric learning problem. In doing so we verify three important design decisions, namely the normalisation, soft maximum function, and projection layers as key ingredients. We theoretically show that the projector implicitly encodes information on past examples, enabling relational gradients for the student. We then show that the normalisation of representations is tightly coupled with the training dynamics of this projector, which can have a large impact on the student's performance. Finally, we show that a simple soft maximum function can be used to address any significant capacity gap problems. Experimental results on various benchmark datasets demonstrate that using these insights can lead to superior or comparable performance to state-of-the-art knowledge distillation techniques, despite being much more computationally efficient. In particular, we obtain these results across image classification (CIFAR100 and ImageNet), object detection (COCO2017), and on more difficult distillation objectives, such as training data efficient transformers, whereby we attain a 77.2% top-1 accuracy with DeiT-Ti on ImageNet.

1. Introduction

Deep neural networks have achieved remarkable success in various applications, ranging from computer vision [30] to natural language processing [53]. However, the high computational cost and memory requirements of deep models have limited their deployment in resource-constrained environments. Knowledge distillation is a popular technique to address this problem through transferring the knowledge of a large teacher model to that of a smaller student model. This technique involves training the student to imitate the output of the teacher, either by directly minimizing the difference between intermediate features or by minimizing the Kullback-Leibler (KL) divergence between their soft predictions. Although knowledge distillation has shown to be very effective, there are still some limitations related to the

computational and memory overheads in constructing and evaluating the losses, as well as an insufficient theoretical explanation for the underlying core principles.

To overcome these limitations, we revisit knowledge distillation from both a function matching and metric learning perspective. We perform an extensive ablation of three important components of knowledge distillation, namely the distance metric, normalisation, and projector network. Alongside this ablation we provide a theoretical perspective and unification of these design principles through exploring the underlying training dynamics. Finally, we extend these principles to a few large scale vision tasks, whereby we achieve comparable or improved performance over state-of-the-art. The most significant result of which pertains to the data-efficient training of transformers, whereby a performance gain of 2.2% is achieved over the best-performing distillation method that are designed explicitly for this task. Our main contributions can be summarised as follows.

1. We explore three distinct design principles from knowledge distillation, namely the projection, normalisation, and distance function. In doing so we demonstrate their unification and coupling with each other, both through analytical means and by observing the training dynamics.
2. We show that a projection layer implicitly encodes relational information from previous samples. Using this knowledge we can remove the need to explicitly construct correlation matrices or memory banks that will inevitably incur a significant memory overhead.
3. We apply the three design principles to image classification, object detection, and data efficient training of transformers to achieve competitive or improved performance over state-of-the-art.

2. Related Work

Knowledge Distillation Knowledge distillation is the process of transferring the knowledge from a large, complex model to a smaller, simpler model. Its usage was originally

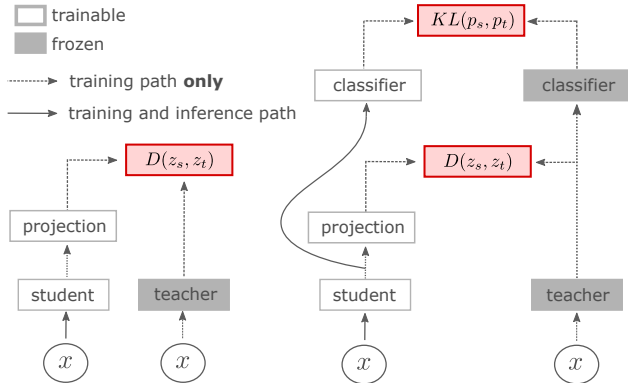


Figure 1: **Training pipeline for knowledge distillation on a classification task.** Left and right show representation distillation with and without the addition of a logit distillation loss respectively. For clarity, the normalisation of arguments for the representation loss D have been omitted.

proposed in the context of image classification [25] whereby the soft teacher predictions would encode relational information between classes. Spherical KD [20] extended this idea by re-scaling the logits, prime aware adaptive distillation [66] introduced an adaptive weighting strategy, while DKD [67] proposed to decouple the original formulation into target class and non-target class probabilities.

Hinted losses [45] were a natural extension of the logit-based approach whereby the intermediate feature maps are used as hints for the student. Attention transfer [60] then proposed to re-weight this loss using spatial attention maps. ReviewKD [7] addressed the problem relating to the arbitrary selection of layers by aggregating information across all the layers using trainable attention blocks. Neuron selectivity transfer [26], similarity-preserving KD [52], and relational KD [40] construct relational batch and feature matrices that can be used as inputs for the distillation losses. Similarly FSP matrices [58] were proposed to extract the relational information through a residual block. In contrast to this theme, we show that a simple projection layer can implicitly capture most relational information, thus removing the need to construct any expensive relational structures.

Representation distillation was originally proposed alongside a contrastive based loss [48] and has since been extended using a Wasserstein distance [6], information theory [38], graph theory [36], and complementary gradient information [68]. Distillation also been empirically shown to benefit from longer training schedules and more data-augmentation [3], which is similarly observed with HSAKD [57] and SSKD [56]. Distillation between CNNs and transformers has also been a very practically motivated task for data-efficient training [51] and has shown to benefit from an ensemble of teacher architectures [44]. However, we show that just a simple extension of some fundamental distillation design principles is much more effective.

Self-Supervised Learning Self-supervised learning (SSL) is an increasingly popular field of machine learning whereby a model is trained to learn a useful representation of unlabelled data. Its popularity has been driven by the increasing cost of manual labelling and has since been crucial for training large transformer models. Various pretext tasks have been proposed to learn these representations, such as image inpainting [22], colorization [64], or prediction of the rotation [18] or position of patches [14, 4]. SimCLR [8] approached self-supervision using a contrastive loss with multi-view augmentation to define the positive and negative pairs. They found a large memory bank of negative representations was necessary to achieve good performance, but would incur a significant memory overhead. MoCo [23] extending this work with a momentum encoder, which was subsequently extended by MoCov2 [11] and MoCov3 [10].

Asymmetric architectures were proposed as an alternative to contrastive learning, whereby no negative samples are needed. Most noticeable works in this area are BYOL [19] and SimSiam [9] which both use stop gradients to avoid representation collapse. DirectPred [49] provided a theoretical understanding of this non-contrastive SSL setting. They introduced a series of conceptual insights into the functional roles of many crucial ingredients used. In doing so they derived a simple linear predictor with competitive performance to some much more complex predictor architectures. In our work we explore knowledge distillation from a similar perspective as DirectPred but observe some unique observations and results pertaining to this distillation setting.

Feature decorrelation is another approach to SSL that avoids the need for negative pairs to address representation collapse. Barlow twins [62] proposed to compute a cross-view correlation matrix and minimise its distance to the identity. This loss was later decomposed into a variance, invariance, and correlation regularisation terms in VICReg [1]. Both contrastive learning and feature decorrelation have since been extended to dense prediction tasks [2] and unified with knowledge distillation [39].

3. Revisiting knowledge distillation

Knowledge distillation (KD) is a technique used to transfer knowledge from a large, powerful model (teacher) to a smaller, less powerful one (student). In the classification setting, it can be done using the soft teacher predictions as pseudo-labels for the student. Unfortunately, this approach does not trivially generalise to non-classification tasks [34] and the classifier may collapse a lot of information [50] that can be useful for distillation. Another approach is to use feature maps from the earlier layers for distillation [45, 60], however, its usage presents two primary challenges: the difficulty in ensuring consistency across different architectures [7] and the potential degradation in the student’s downstream performance for cases where the inductive biases of

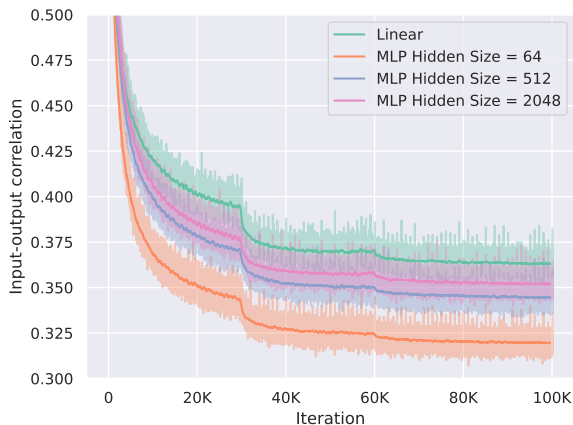


Figure 2: **Correlation between input-output features using different projector architectures.** All projector architectures considered will gradually decorrelate the input-output features. Although this decorrelation is attributed to the layer destroying irrelevant information, it can degrade the efficacy of distilling through to the student backbone.

the two networks differ [48] A compromise, which strikes a balance between the two approaches discussed above, is to distill the representation directly before the output space. Representation distillation has been successfully adopted in past works [48, 68, 38] and is the focus of this paper. The exact training framework used is described in figure 1 alongside an extension to incorporate a logit distillation loss. The projection layer shown was originally used to simply match the student and teacher dimensions [45], however, we will show that its role is much more important and it can lead to significant performance improvements even when the two feature dimensions match. The two representations are also typically both followed by some normalisation scheme as a way of appropriately scaling the gradients. However, we find this normalisation has a more interesting property in its relation to what information is encoded in the learned projector weights.

In this work we provide a theoretical perspective to motivate some simple and effective design choices for knowledge distillation. In contrast to the recent works [52, 38], we show that an explicit construction of complex relational structures, such as feature kernels [21] is not necessary. In fact, most of this structure can be learned implicitly through the tightly coupled interaction of a learnable projection layer and an appropriate normalisation scheme. In the following we discuss the importance of multi-view augmentation in distillation. We subsequently investigate the training dynamics of the projection layer with the normalisation scheme. We explore the impact and trade-offs that arise from the architecture design of the

Description	Repulsive force	acc@1
KD	$KL(p_s \parallel p_t)$	71.37
Mean-square	$\ z_s - z_t\ _2^2$	71.08
no projection		
Mean-square	$\ z_s - z_t\ _2^2$	71.53
Batch-normalised	$\ BN(z_s) - BN(z_t)\ _2^2$	71.34
Correlation	$\ BN(z_s) \cdot BN(z_t) - \mathbf{1}\ _2^2$	71.35
Higher-order	$\ BN(z_s) \cdot BN(z_t) - \mathbf{1}\ _4^4$	71.31
Soft maximum	$\log \sum \ BN(z_s) \cdot BN(z_t) - \mathbf{1}\ _4^4$	71.63

Table 1: **Ablating the importance in the choice of metric function** using a ResNet34 and a ResNet18 student on the ImageNet dataset. The loss modifications are highlighted in red and vanilla KD is provided as a reference.

projector. Finally, we propose a simple modification to the distance metric to address issues arising from a large capacity gap between the student and teacher models.

Importance of multi-view augmentation. Knowledge distillation can be viewed as a form of function matching. This perspective motivates the intuition behind long training schedules and more aggressive augmentations in an attempt to densely sample the domain. This principle has been extensively covered by Beyer *et al.* [3] and has motivated our modification to the CIFAR100 distillation benchmark provided by CRD [48] In doing so we introduce a multi-view augmentation strategy, from which we report our results and reproduce those from other recent distillation methods. These results can be seen in table 5 and show that significant improvements can be made to even standard logit distillation through introducing a wider set of augmentations. All other settings, such as the optimiser, learning rate schedule, and number of epochs, are maintained the same.

The projection weights encode relational information from previous samples. The projection layer plays a crucial role in KD as it provides an implicit encoding of previous samples and its weights can capture the relational information needed to transfer information regarding the correlation between features. Table 1 shows the difference a single linear projector layer makes when combined with a simple L2 loss. This improvement suggests that this layer's role in distillation can be described more concisely as being an encoder of essential information needed for the distillation loss itself. Most recent works propose a manual construction of some relational information to be used as part of a loss [40, 52], however, we posit that an implicit and learnable approach is much more effective. To explore this phenomenon in more detail, we consider the update equations for the projector weights and its training dynamics. Without loss in generality, consider a simple L2 loss and a linear projection layer without any bias term.

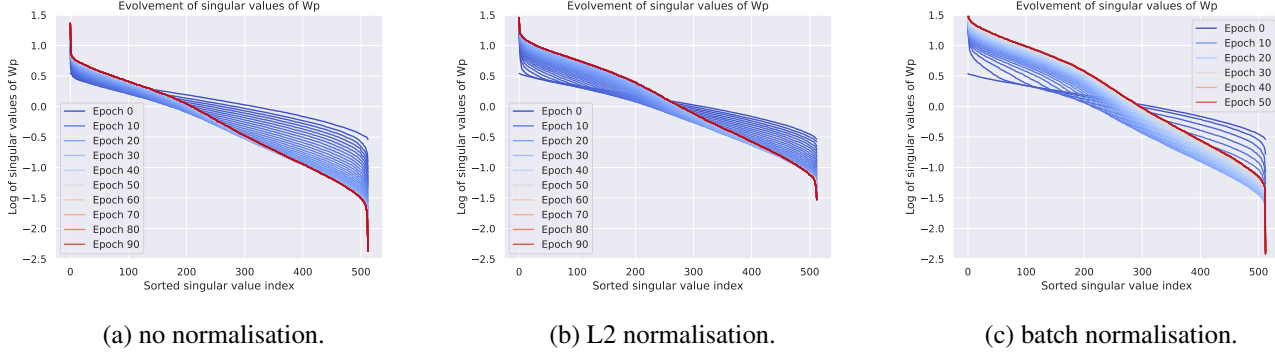


Figure 3: **Evolution of singular values of the projection weights \mathbf{W}_p under three different representation normalisation schemes.** The student is a Resnet-18, while the teacher is a ResNet-50. The three curves shows the evolution of singular values for the projector weights when the representations undergo no normalisation, L2 normalisation, and batch norm respectively.

$$D(\mathbf{W}_p) = \frac{1}{2} \|\mathbf{Z}_s \mathbf{W}_p - \mathbf{Z}_t\|_2^2 \quad (1)$$

Using the trace property of the Frobenius norm, we can express this loss as follows:

$$D(\mathbf{W}_p) = \frac{1}{2} \text{tr} \left((\mathbf{Z}_s \mathbf{W}_p - \mathbf{Z}_t)^T (\mathbf{Z}_s \mathbf{W}_p - \mathbf{Z}_t) \right) \quad (2)$$

$$= \frac{1}{2} \text{tr} (\mathbf{W}_p^T \mathbf{Z}_s^T \mathbf{Z}_s \mathbf{W}_p - \mathbf{Z}_t^T \mathbf{Z}_s \mathbf{W}_p \quad (3)$$

$$- \mathbf{W}_p^T \mathbf{Z}_s^T \mathbf{Z}_t + \mathbf{Z}_t^T \mathbf{Z}_t) \quad (4)$$

Taking the derivative with respect to \mathbf{W}_p

$$\dot{\mathbf{W}}_p = - \frac{\partial D(\mathbf{W}_p)}{\partial \mathbf{W}_p} \quad (5)$$

$$= -\mathbf{Z}_s^T \mathbf{Z}_s \mathbf{W}_p + \mathbf{Z}_s^T \mathbf{Z}_t \quad (6)$$

The update rule can then be simplified

$$\dot{\mathbf{W}}_p = \mathbf{C}_{st} - \mathbf{C}_s \mathbf{W}_p \quad (7)$$

where $\mathbf{C}_s = \mathbf{Z}_s^T \mathbf{Z}_s \in \mathbb{R}^{d_s \times d_s}$ and $\mathbf{C}_{st} = \mathbf{Z}_s^T \mathbf{Z}_t \in \mathbb{R}^{d_s \times d_t}$ denote self and cross correlation matrices that capture the relationship between features. Due to the capacity gap between the student network and the teacher network, there is no linear projection between these two representation spaces. Instead, the projector will converge on an approximate mapping that we later show is governed by the normalisation being employed. However, we note that, unlike in self-supervised learning, this solution will never be unstable since representation collapse is not possible - the teacher is frozen and we jointly trained with the ground truth.

Whitened features: consider using self-supervised learning in conjunction with distillation whereby the student features are whitened to have perfect decorrelation [15], or

alternatively, they are batch normalised and sufficiently regularised with a feature decorrelation term [1]. In this setting, the fixed point solution for the projection weights will be symmetric and will capture the cross relationship between student and teacher features.

$$\mathbf{C}_{st} - \mathbf{C}_s \mathbf{W}_p = 0 \quad \text{where } \mathbf{C}_s = \mathbf{I} \quad (8)$$

$$\rightarrow \mathbf{W}_p = \mathbf{C}_{st} \quad (9)$$

Other normalisation schemes, such as those that jointly normalise the projected features and the teacher features, will have a much more involved analysis but will unlikely provide any additional insight on the dynamics of training itself. Thus, we propose to explore the training trajectories of the projector weights singular values. This will help quantify how the projector is mapping the student features to the teachers space. We cover this in the next section along with additional insights into what is being learned and distilled.

The choice of normalisation directly affects the training dynamics of \mathbf{W}_p . Equation 7 shows that the projector weights can encode relational information between the student and teacher's features. This suggests redundancy in explicitly constructing and updating a large memory bank of previous representations [48]. By considering a weight decay η and a learning rate α_p , the update equation can be given as follows:

$$\mathbf{W}_p \rightarrow \mathbf{W}_p + \alpha_p \dot{\mathbf{W}}_p - \eta \mathbf{W}_p \quad (10)$$

$$= (1 - \eta) \mathbf{W}_p + \alpha_p \dot{\mathbf{W}}_p \quad (11)$$

By setting $\eta = \alpha_p$ we can see that the projection layer will reduce to a moving average of relational features, which is very similar to the momentum encoder used by CRD [48].

Other works suggest to extract relational information on-the-fly by constructing correlation or gram matrices [38, 41]. We show that this is also not necessary and more complex information can be captured through careful design of the projector architecture. We also demonstrate that, in general, the use of a projector will scales much more favourably for larger batch sizes and feature dimensions. We also note that the handcrafted design of kernel functions [28, 21, 38] may not generalise to large scale or complex real-world datasets.

Description	Equation	acc@1
Batch Norm [27]	$\frac{z_{i,k} - \mu_k}{\sqrt{\sigma_k + \epsilon}}$	62.76
L2	$\frac{z}{\ z\ _2}$	57.07
Group Norm [55] groups = 16	$\frac{z_{i,k} - \mu_{i,s_k}}{\sqrt{\sigma_{i,s_k} + \epsilon}}$	59.35
↳ w/ Weight Norm [42]		56.41

Table 2: **Ablating the importance in the normalisation** using a ResNet50 teacher and a ResNet18 student in the few-shot distillation setting on ImageNet.

From the results in table 2, we observe that when fixing all other settings, the choice of normalisation can significantly affect the student’s performance. To explore this in more detail, we consider the training trajectories of \mathbf{W}_p under different normalisation schemes. We find that the choice of normalisation not only controls the training dynamics, but also the fixed point solution (see equation 7). We argue that the efficacy of distillation is dependent on how much relational information can be encoded in the learned weights and how much information is lost through the projection. To jointly evaluate these two properties we show the evolution of singular values of the projector weights during training. The results can be seen in figure 3 and show that the better performing normalisation methods (table 2) are shrinking far fewer singular values towards zero. This shrinkage can be described as collapsing the input along some dimension, which will induce some information loss and it is this information loss that degenerates the efficacy of distillation.

Larger projector networks learn to decorrelate the input-output features. One natural extension of the previous observations is to use a larger projector network to encode more information relevant for the distillation loss. Unfortunately, we observe that a trivial expansion of the projection architecture does not necessarily improve the students performance (see table 4). To explain this observation we evaluate a measure of decorrelation between the input and output features of these projector networks. The results can be seen in figure 2 and we can see that the larger projectors learn to decorrelate more and more features from the input. This decorrelation can lead to the

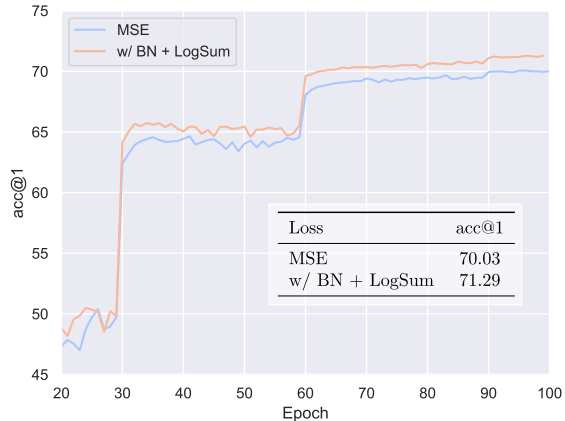


Figure 4: **KD with a large capacity gap.** Top-1 accuracy (%) using a ResNet18 student and a ResNet50 teacher. Experiments were both performed with a linear projection.

projector learning features that are not shared with the student backbone, which will subsequently diminish the effectiveness of distillation. These observations suggest that there is an inherent trade-off between the projector capacity and the efficacy of distillation. We do expect that some careful handcrafted design of the projector architectures could provide a more favourable trade-off, which agrees with the reported results using a projector ensemble [12]. However, in favour of simplicity, we use a linear projector for all of the larger scale evaluations.

The soft maximum function can address distilling across a large capacity gap. When the capacity gap between the student and the teacher is large, representation distillation can become challenging. More specifically, the student network may have insufficient capacity to perfectly align these two spaces and in attempting to do so may degrade its downstream performance. To address this issue we explore the use of a soft maximum function which will soften the contribution of relatively close matches in a batch. In this way the loss can be adjusted to compensate for poorly aligned features which may arise when the capacity gap is large. The family of functions which share these properties can be more broadly defined through a property of their gradients. In favour of simplicity, we use the simple *LogSum* function throughout our experiments.

$$f(\mathbf{x}) = \log \sum_i x_i^\alpha \tag{12}$$

where α is a smoothing factor. We also note that other functions, such as the *LogSumExp*, with a temperature parameter τ , have been used in SimCLR and CRD to a similar effect. Figure 4 shows our empirical observations

	Teacher	Student	AT [60]	KD [25]	SP [52]	CC [41]	CRD [25]	ReviewKD [7]	Ours
acc@1	26.69	30.25	29.30	29.34	29.38	30.04	28.62	28.39	28.37
acc@5	8.58	10.93	10.00	10.12	10.20	10.83	9.51	9.42	9.41

Table 3: **Top-1 and Top-5 error rates (%) on ImageNet.** ResNet18 as student, ResNet34 as teacher.

using a large capacity gap with and without the addition of both a normalisation and soft maximum operator. The improvements are much more significant in this case than for the small capacity gap (table 1).

In table 1 we also perform an additional ablation on the impact of a few heuristically derived distance functions. We observe, on the large-scale ImageNet benchmark, there is little to no benefit in varying the underlying function, but significant improvements can be made by introducing a linear projection or a soft maximum operator in conjunction with normalisation. As discussed previously this latter improvement is amplified when the capacity gap between the two models increases.

Projector	acc@1
Linear	59.75
MLP	
↳ Hidden Size = 64	58.64
↳ Hidden Size = 512	59.49
↳ Hidden Size = 2048	59.54

Table 4: **Ablating the importance in the projector** using a ResNet34 teacher and a ResNet18 student in the few-shot distillation setting on ImageNet.

4. Benchmark evaluation

Implementation details. We follow the same training schedule as CRD [48] for both the CIFAR100 and ImageNet experiments. For the object detection, we use the same training schedule as ReviewKD [7], while for the data efficient training we use the same as Co-Advice [44]. All experiments were performed on a single NVIDIA RTX A5000. When using batch normalisation for the representations, we removed the affine parameters and set $\epsilon = 0.0001$.

4.1. Classification on CIFAR100 and ImageNet

Experiments on the CIFAR-100 classification task [29] consist of 60K 32x32 RGB images across 100 classes with a 5:1 training/testing split. Table 5 shows the results for several student-teacher pairings. To enable a fair evaluation, we have only included the methods that use the same teacher weights provided by SSKD[56]. In these experiments we use an MLP projector with a hidden size of 1024 and no additional KL divergence loss. We observe that not only is the choice of augmentation critical for good performance on

this dataset, but applying our principles can attain state-of-the-art across most architecture pairs. The most significant improvements pertain to the cross-architecture experiments or where the capacity gap is large.

The ImageNet [46] classification uses 1.3 million images that are classified into 1000 distinct classes. The input size are set to 224 x 224, and we employed a typical augmentation procedure that includes cropping and horizontal flipping. We used the torchdistill library with the standard configuration, which involves 100 training epochs using SGD and an initial learning rate of 0.1, which is decreased by a factor of 10 at epochs 30, 60, and 90. The results can be seen in table 3 and although the choice of architectures is not in favour of our method since the capacity gap is small, we are still able to attain competitive performance. Other methods, such as ICKD [33] or SimKD [5] either modify the original training settings or modify the underlying student architecture, and so have been omitted from this evaluation.

4.2. Object Detection on COCO

We extend the application of our method to object detection, whereby we employ a similar approach as used in the classification task by distilling the backbone output features of both the student and teacher networks. To evaluate the efficacy of our method, we conduct experiments on the widely-used COCO2017 dataset [32] under the same settings provided in ReviewKD. We then further demonstrate the applicability of our distillation principles on the more recent and efficient YOLOv5 model [69]. In both cases we show improved student performance on the downstream task, whereby competitive performance is achieved with ReviewKD despite being significantly simpler and cheaper to integrate into a given distillation pipeline. Our method even outperforms FPGI [54], which is directly designed for detection.

4.3. Data efficient training for transformers

Transformers have emerged as a viable replacement for convolution-based neural networks (CNN) in visual learning tasks. Despite the promise of these models, their performance will suffer when there is insufficient training data available, such as in the case of ImageNet. DeiT [51] was the first to address this problem through the use of knowledge distillation. Although the authors show improved alignment with the teacher, we believe this fails to capture why less data is needed.

Teacher	wrn40-2	wrn40-2	resnet56	resnet32x4	vgg13	ResNet50	ResNet50	resnet32x4	resnet32x4	wrn40-2
Student	wrn16-2	wrn40-1	resnet20	resnet8x4	MobileNetV2	MobileNetV2	vgg8	ShuffleV1	ShuffleV2	ShuffleV1
Teacher	76.46	76.46	73.44	79.63	75.38	79.10	79.10	79.63	79.63	76.46
Student	73.64	72.24	69.63	72.51	65.79	65.79	70.68	70.77	73.12	70.77
KD [25]	74.92	73.54	70.66	73.33	67.37	67.35	73.81	74.07	74.45	74.83
FitNet [45]	75.75	74.12	71.60	74.31	68.58	68.54	73.84	74.82	75.11	75.55
AT [60]	75.28	74.45	71.78	74.26	69.34	69.28	73.45	74.76	75.30	75.61
CRD [48]	76.04	75.52	71.68	75.90	68.49	70.32	74.42	75.46	75.72	75.96
SSKD [56]	76.04	76.13	71.49	76.20	71.53	72.57	75.76	78.44	78.61	77.40
Our Method	76.14	75.42	71.75	76.44	71.47	72.81	76.20	77.32	79.06	79.22
KD [†] [25]	75.94	75.32	71.10	75.84	70.79	71.29	75.75	77.80	78.43	78.00
CRD [†] [48]	77.27	76.15	72.21	77.69	71.65	72.03	75.73	78.57	79.01	78.54
DKD [†] [67]	74.96	75.89	70.95	77.52	72.01	73.30	76.88	79.71	80.08	77.86
Our Method	77.61	76.04	72.25	78.37	72.82	73.51	77.08	78.99	79.86	78.79

Table 5: **KD between Similar and Different Architectures.** Top-1 accuracy (%) on CIFAR100. **Bold** is used to denote the best results. All reported models are trained using pairs of augmented images. Those reported in the **orange** box use RandAugment [13] strategy, while those in the **green** box use pre-defined rotations, as used in SSKD. [†] denotes reproduced results in a new augmentation setting using the authors provided code.

Model	mAP (50-95)	mAP 50	params	FLOPs
YOLOv5m (teacher)	64.1	45.4	21.2	49.0
YOLOv5s	56.8	37.4	7.2	16.5
w/ Our Method	57.3	37.5		
	mAP	AP50	params	
Faster R-CNN w/ R50-FPN (teacher)	40.22	61.02	41.7	
Faster R-CNN w/ MV2-FPN	29.47	48.87	23.4	
w/ KD [25]	30.13	50.28		
w/ FitNet [45]	30.20	49.80		
w/ FPGI [54]	31.16	50.68		
w/ ReviewKD [7]	33.71	53.15		
w/ Our Method	<u>32.92</u>	<u>52.96</u>		

Table 6: **Object detection on COCO.** (top) We report the standard COCO metric of mAP averaged over IOU thresholds in [0.5 : 0.05 : 0.95] along with the standard PASCAL VOC’s metric [16], which is the average mAP@0.5. (bottom) For the R-CNN results, we report the mAP and AP50 metrics to enable a consistent comparison with ReviewKD.

We posit that the distillation process encourages the student to learn layers which are "more" translational equivariant in attempt to match the teacher’s underlying function. Although this is the principle that motivates using an ensemble of teacher models with different inductive biases [44], there is still no thorough demonstration on if the inductive biases are actually being transferred. In this section we attempt to address this gap by introducing a measure of equivariance. We show that applying our distillation principles to this task can achieve significant improvements over state-of-the-art as a result of transferring more of the translational equivariance.

The results of these experiments are shown in table 7. We use the exact same training methodology as co-advice [44]

and choose to use batch normalisation, a linear projection layer, and $\alpha = 4$ as the parameters for distillation. We observe a significant improvement over both DeiT and CivT when the capacity gap is large. However, as the capacity gap diminishes, and the student approaches the same performance as the teacher, this improvement is much less significant. Multiple factors, such as the soft maximum function and the batch normalisation, will be contributing to this observed result. However, the explanation is more concisely described by the fact that our distillation loss transfers more translational equivariance, which is discussed in the next section.

Cross architecture distillation can implicitly transfer inductive biases. CNNs use convolutions, which are spatially local operations, whereas transformers use self-

attention, which are global operations. We expect that a benefit of this cross-architecture distillation setting is that the students learn to be "more" spatially equivariant in an attempt to match the teachers underlying function. It is this strong inductive bias that can reduce the amount of training data needed. A layer is translation equivariant if the following property holds:

$$\phi(T\mathbf{x}) = T\phi(\mathbf{x}) \quad (13)$$

In other words, if we take a translated input $T\mathbf{x}$ and pass it through a layer ϕ , the result should be equivalent to first applying ϕ to \mathbf{x} and then performing the translation. A natural measure of equivariance can then be the difference between the left and right-hand side of this equation 13.

$$\mu_T(\phi) = \|\phi(T\mathbf{x}) - T\phi(\mathbf{x})\|_2^2 \quad (14)$$

We evaluate this measure on a block of self-attention layers by first removing the distillation and class tokens and then rolling the patch tokens to recover the spatial dimensions. This operation can then be performed on the input and output tensors before applying a translation. Figure 5 shows how this measure of equivariance evolves over the course of training. In general, we observe that the distilled models do in fact learn to preserve spatial locality between feature maps, which aligns with the function matching perspective for distillation (see figure 5). We also find that our distillation method can transfer a lot more of this equivariance property to the student, where we find that the undistilled models have values of μ_T in the range of [1.4, 1.9]. Although CivT-S does learn this spatial locality to some extent, it is much less pronounced than our distilled model despite both models achieving similar accuracy.

Network	acc@1	acc@5	#params
RegNety 160 [43] (teacher)	82.6	96.4	84M
CivT-Ti [44]	74.9	-	6M
DeiT-Ti [51]	72.2	91.1	5M
w/ KD [51]	74.5	91.9	6M
w/ Our Method	77.1	93.7	6M
CivT-S [44]	82.0	-	22M
DeiT-S [51]	79.8	95.0	22M
w/ KD [51]	81.2	95.4	22M
w/ Our Method	82.1	96.0	22M

Table 7: **Data-efficient training of transformers** on Imagenet with DeiT. All models are trained for 300 epochs using mixup [63].

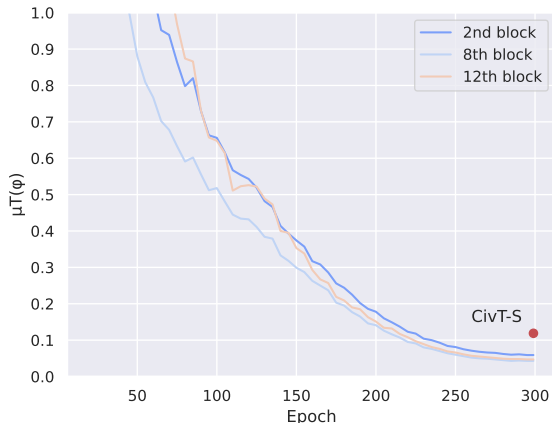


Figure 5: **Measure of translational equivariance of a DeiT-S transformer model trained with our distillation.** Reported measure was computed after every epoch and averaged over 256 images. We observe that distillation can indeed transfer inductive biases, which enables data-efficient training.

5. Conclusion

In this paper, we revisited knowledge distillation from a function matching and metric learning perspective. We performed an extensive ablation on the most effective and scalable components of distillation and in doing so provide a theoretical perspective to understand these observations. By extending these principles to a wide range of tasks, we achieve competitive or improved performance to state-of-the-art across image classification, object detection, and data efficient training of transformers. Although we do not aim to necessarily propose a new method, we do provide an effective theory to approach the capacity gap problem in distillation. We also significantly reduce the complexity and memory consumption’s of existing pipelines through unifying a new underlying principle of distillation. Looking ahead to future research in this area, we expect to see the joint development of more sophisticated normalisation schemes and projection networks, which will encode more complex and informative features for the distillation process.

Code Reproducibility. To facilitate the reproducibility of results, we will release all the training code and pre-trained weights. The ImageNet experiments are also performed using the popular *torchdistill* [37] framework, while the CIFAR100 and data-efficient training code is based on those provided by CRD [48] and co-advice [44].

References

- [1] Adrien Bardes, Jean Ponce, and Yann LeCun. “VICReg: Variance-Invariance-Covariance Regularization for Self-Supervised Learning”. In: *ICLR* (2022).
- [2] Adrien Bardes, Jean Ponce, and Yann LeCun. “VICRegL: Self-Supervised Learning of Local Visual Features”. In: *NeurIPS* (Oct. 2022).
- [3] Lucas Beyer et al. “Knowledge distillation: A good teacher is patient and consistent”. In: *CVPR* (2022).
- [4] Fabio M. Carlucci et al. “Domain Generalization by Solving Jigsaw Puzzles”. In: *CVPR* (2019).
- [5] Defang Chen et al. “Knowledge Distillation with the Reused Teacher Classifier”. In: *CVPR* (2022).
- [6] Liqun Chen et al. “Wasserstein Contrastive Representation Distillation”. In: *CVPR* (2020).
- [7] Pengguang Chen et al. “Distilling Knowledge via Knowledge Review”. In: *CVPR* (2021).
- [8] Ting Chen et al. “A simple framework for contrastive learning of visual representations”. In: *ICML* (2020).
- [9] Xinlei Chen and Kaiming He. “Exploring Simple Siamese Representation Learning”. In: *CVPR* (2021).
- [10] Xinlei Chen, Saining Xie, and Kaiming He. “An Empirical Study of Training Self-Supervised Vision Transformers”. In: *ICCV* (Apr. 2021).
- [11] Xinlei Chen et al. “Improved Baselines with Momentum Contrastive Learning”. In: *arXiv preprint* (Mar. 2020).
- [12] Yudong Chen et al. “Improved Feature Distillation via Projector Ensemble”. In: *NeurIPS* (2022).
- [13] Ekin D. Cubuk et al. “RandAugment: Practical automated data augmentation with a reduced search space”. In: *CVPR Workshop* (2020).
- [14] Carl Doersch, Abhinav Gupta, and Alexei A. Efros. “Unsupervised Visual Representation Learning by Context Prediction”. In: *ICCV* (May 2015).
- [15] Aleksandr Ermolov et al. “Whitening for Self-Supervised Representation Learning”. In: *ICML* (July 2020).
- [16] Mark Everingham et al. “The PASCAL Visual Object Classes (VOC) Challenge”. In: *IJCV* (2010).
- [17] Michael H. Fox, Kyungmee Kim, and David Ehrenkrantz. “MobileNetV2: Inverted Residuals and Linear Bottlenecks”. In: *CVPR* (2018).
- [18] Spyros Gidaris, Praveer Singh, and Nikos Komodakis. “Unsupervised Representation Learning by Predicting Image Rotations”. In: *ICLR* (Mar. 2018).
- [19] Jean Bastien Grill et al. “Bootstrap your own latent a new approach to self-supervised learning”. In: *NeurIPS* (2020).
- [20] Jia Guo et al. “Reducing the Teacher-Student Gap via Spherical Knowledge Distillation”. In: *arXiv preprint* (2020).
- [21] Bobby He and Mete Ozay. “Feature Kernel Distillation”. In: *ICLR* (2022).
- [22] Kaiming He et al. “Masked Autoencoders Are Scalable Vision Learners”. In: *CVPR* (Nov. 2022).
- [23] Kaiming He et al. “Momentum Contrast for Unsupervised Visual Representation Learning”. In: *CVPR* (Nov. 2020).
- [24] Kaiming He et al. “ResNet - Deep Residual Learning for Image Recognition”. In: *CVPR* (2015).
- [25] Geoffrey Hinton, Oriol Vinyals, and Jeff Dean. “Distilling the Knowledge in a Neural Network”. In: *NeurIPS* (2015).
- [26] Zehao Huang and Naiyan Wang. “Like What You Like: Knowledge Distill via Neuron Selectivity Transfer”. In: *arXiv preprint* (2017).
- [27] Sergey Ioffe and Christian Szegedy. “Batch Normalization: Accelerating Deep Network Training by Reducing Internal Covariate Shift”. In: *arXiv preprint* (2015).
- [28] Chaitanya K. Joshi et al. “On Representation Knowledge Distillation for Graph Neural Networks”. In: *arXiv preprint* (Nov. 2021).
- [29] Alex Krizhevsky. “Learning Multiple Layers of Features from Tiny Images”. In: (2009).
- [30] Alex Krizhevsky, Ilya Sutskever, and Geoffrey E Hinton. “ImageNet Classification with Deep Convolutional Neural Networks”. In: *NeurIPS* (2012).
- [31] Shanda Li et al. “Can Vision Transformers Perform Convolution?” In: *arXiv preprint* (Nov. 2021).
- [32] Tsung Yi Lin et al. “Microsoft COCO: Common objects in context”. In: *ECCV* (2014).
- [33] Li Liu et al. “Exploring Inter-Channel Correlation for Diversity-preserved Knowledge Distillation”. In: *ICCV* (2021).
- [34] Yifan Liu et al. “Structured Knowledge Distillation for Semantic Segmentation”. In: *CVPR* (2019).
- [35] Ningning Ma et al. “Shufflenet V2: Practical guidelines for efficient cnn architecture design”. In: *Lecture Notes in Computer Science*. 2018.
- [36] Yuchen Ma, Yanbei Chen, and Zeynep Akata. “Distilling Knowledge from Self-Supervised Teacher by Embedding Graph Alignment”. In: *Bmvc* (Nov. 2022).

- [37] Yoshitomo Matsubara. “torchdistill : A Modular, Configuration-Driven Framework for Knowledge Distillation”. In: (2020).
- [38] Roy Miles, Adrian Lopez Rodriguez, and Krystian Mikolajczyk. “Information Theoretic Representation Distillation”. In: *BMVC* (Dec. 2022).
- [39] Roy Miles et al. “MobileVOS: Real-Time Video Object Segmentation Contrastive Learning meets Knowledge Distillation”. In: *CVPR* (Mar. 2023).
- [40] Wonpyo Park et al. “Relational Knowledge Distillation”. In: *CVPR* (2019).
- [41] Baoyun Peng et al. “Correlation congruence for knowledge distillation”. In: *CVPR* (2019).
- [42] Siyuan Qiao et al. “Micro-Batch Training with Batch-Channel Normalization and Weight Standardization”. In: *arXiv preprint* (Mar. 2019).
- [43] Ilija Radosavovic et al. “Designing Network Design Spaces”. In: *CVPR* (Mar. 2020).
- [44] Sucheng Ren et al. “Co-advise: Cross Inductive Bias Distillation”. In: *CVPR* (2022).
- [45] Adriana Romero et al. “FitNets: Hints For Thin Deep Nets”. In: *ICLR* (2015).
- [46] Olga Russakovsky et al. “ImageNet Large Scale Visual Recognition Challenge”. In: *IJCV* (2014).
- [47] Karen Simonyan and Andrew Zisserman. “Very Deep Convolutional Networks For Large-scale Image Recognition”. In: *ICLR* (2015).
- [48] Yonglong Tian, Dilip Krishnan, and Phillip Isola. “Contrastive representation distillation”. In: *ICLR* (2019).
- [49] Yuandong Tian, Xinlei Chen, and Surya Ganguli. “Understanding self-supervised Learning Dynamics without Contrastive Pairs”. In: *ICML* (2021).
- [50] Naftali Tishby. “Deep Learning and the Information Bottleneck Principle”. In: *IEEE Information Theory Workshop (ITW)* (2015).
- [51] Hugo Touvron et al. “Training data-efficient image transformers & distillation through attention”. In: *PMLR* (2021).
- [52] Fred Tung and Greg Mori. “Similarity-preserving knowledge distillation”. In: *ICCV* (2019).
- [53] Ashish Vaswani et al. “Attention Is All You Need”. In: *NeurIPS* (June 2017).
- [54] Tao Wang et al. “Distilling Object Detectors with Fine-grained Feature Imitation”. In: *CVPR* (June 2019).
- [55] Yuxin Wu and Kaiming He. “Group Normalization”. In: *arXiv preprint* (Mar. 2018).
- [56] Guodong Xu et al. “Knowledge Distillation Meets Self-supervision”. In: *ECCV* (2020).
- [57] Chuanguang Yang et al. “Hierarchical Self-supervised Augmented Knowledge Distillation”. In: *IJCAI* (2021).
- [58] Junho Yim. “A Gift from Knowledge Distillation: Fast Optimization, Network Minimization and Transfer Learning”. In: *CVPR* (2017).
- [59] Chulhee Yun et al. “Are Transformers universal approximators of sequence-to-sequence functions?” In: *ICLR* (2020).
- [60] Sergey Zagoruyko and Nikos Komodakis. “Paying more attention to attention: Improving the performance of convolutional neural networks via attention transfer”. In: *ICLR*. 2019.
- [61] Sergey Zagoruyko and Nikos Komodakis. “Wide Residual Networks”. In: *BMVC* (2016).
- [62] Jure Zbontar et al. “Barlow Twins: Self-Supervised Learning via Redundancy Reduction”. In: *ICML* (2021).
- [63] Hongyi Zhang et al. “Mixup: Beyond empirical risk minimization”. In: *ICLR* (2017).
- [64] Richard Zhang, Phillip Isola, and Alexei A. Efros. “Colorful Image Colorization”. In: Mar. 2016.
- [65] Xiangyu Zhang, Xinyu Zhou, and Mengxiao Lin. “ShuffleNet: An Extremely Efficient Convolutional Neural Network for Mobile Devices”. In: *CVPR* (2018).
- [66] Youcai Zhang et al. “Prime-Aware Adaptive Distillation”. In: *ECCV* (2020).
- [67] Borui Zhao, Renjie Song, and Yiyu Qiu. “Decoupled Knowledge Distillation”. In: *CVPR* (2022).
- [68] Jinguo Zhu et al. “Complementary Relation Contrastive Distillation”. In: *CVPR* (2021).
- [69] Xingkui Zhu et al. “TPH-YOLOv5: Improved YOLOv5 Based on Transformer Prediction Head for Object Detection on Drone-captured Scenarios”. In: *VisDrone ICCV workshop* (Aug. 2021).

6. Supplementary Material

6.1. Few-shot distillation experiments

Due to the limited compute resources available, we were unable to perform some ablation experiments using the full ImageNet training data. To address this concern, and to avoid using a poor surrogate dataset (i.e. CIFAR100), we propose a more difficult few-shot distillation setting. In this setting, the models are still trained and evaluated on the large-scale ImageNet dataset, but with only a subset of the training data available. This results in the distillation objective being much more challenging. In all of these experiments we sample the same 20% of images from each class to ensure the overall class balance is maintained.

6.2. Measure of translational equivariance

In this section we provide more details on the proposed measure of translational equivariance and the motivation for its usage. In the cross inductive-bias distillation literature it is common to evaluate the effectiveness of a distillation pipeline through a measure of agreement between the student and the teacher [51, 44]. We argue that this metric fails to encapsulate why one distillation method is more data efficient than another. We hypothesise that the most effective cross architecture distillation methods are those that transfer most of the inductive biases. To verify this claim, we introduce a measure of equivariance and show that a good distillation loss does indeed minimise this. For the convolution \rightarrow transformer distillation setting, the most appropriate choice of measure is a measure of translational equivariance. This is because the teacher will have this equivariance explicitly enforced through the underlying convolutional layers, whereas the self-attention student will not. Recent works have shown that the self-attention layer can, in principle, learn the same operation as a convolution [31]. The authors then show that injecting this bias will improve the data-efficiency, however, we show that this is not necessary since the bias can be learned implicitly through distillation.

Self-attention layers are known to be permutation equivariant. However, with the use of additive positional encodings, this restriction can be relaxed and can enable these layers to learn any arbitrary sequence-to-sequence function [59]. When we apply transformers to the vision domain, the tokens are provided as non-overlapping patches of the image. Thus, to perform a spatial translation on the sequence of tokens, we must first roll the sequence back to have the $H \times W$ dimensions in the same way in which we unrolled it at the input. The exact details can be seen in algorithm 1. Using this defined measure, we find that non-distilled transformers are over $15\times$ less equivariant than their distilled counterparts.

Algorithm 1 Translational equivariance measure

```
1: # x: Image representation B x N x C
2: # T: Spatial translation
3: # blk: Block of self-attention layers
4: def compute(x, T):
5:     # 14 x 14 patches
6:     h = 14
7:     w = 14
8:     b, n, c = x.shape
9:
10:    # remove positional encodings
11:    xp = x[:, 2:]
12:
13:    # roll token-dim into H x W dimensions
14:    xp = xp.transpose(1, 2).reshape(b, c, h, w)
15:    Tx = T(xp)
16:
17:    # unroll H x W dimensions
18:    Tx = Tx.flatten(2).transpose(1, 2)
19:
20:    # add back the positional encodings
21:    Tx = torch.cat((x[:, 0:2], Tx), dim=1)
22:
23:    # forward pass with and without an input
    # translation
24:    Fx = blk(x)
25:    FTx = blk(Tx)
26:
27:    # remove position encoding
28:    Fxp = Fx[:, 2:]
29:    b, n, c = Fxp.shape
30:
31:    Fxp = Fxp.transpose(1, 2).reshape(b, c, h, w)
32:    TFxp = T(Fxp)
33:    TFxp = TFxp.flatten(2).transpose(1, 2)
34:
35:    # add back position encoding
36:    TFx = torch.cat((x[:, 0:2], TFxp), dim=1)
37:
38:    return F.mse_loss(TFxp, FTx)
```

6.3. Model Architectures

In experiments, we use the following model architectures.

- Wide Residual Network (WRN) [61]: WRN- $d-w$ represents wide ResNet with depth d and width factor w .
- resnet [24]: We use ResNet-d to represent CIFAR-style resnet with 3 groups of basic blocks, each with 16, 32, and 64 channels, respectively. In our experiments, resnet8x4 and resnet32x4 indicate a 4 times wider network (namely, with 64, 128, and 256 channels for each of the blocks).
- ResNet [24]: ResNet-d represents ImageNet-style ResNet with bottleneck blocks and more channels.
- MobileNetV2 [17]: In our experiments, we use a width multiplier of 0.5.
- vgg [47]: The vgg networks used in our experiments are adapted from their original ImageNet counterpart.
- ShuffleNetV1 [65], ShuffleNetV2 [35]: ShuffleNets are proposed for efficient training and we adapt them to input of size 32x32.

Implementation Details. All methods evaluated in our experiments use SGD. For CIFAR-100, we initialize the learning rate as 0.05, and decay it by 0.1 every 30 epochs after the first 150 epochs until the last 240 epoch. For MobileNetV2, ShuffleNetV1 and ShuffleNetV2, we use a learning rate of 0.01 as this learning rate is optimal for these models in a grid search, while 0.05 is optimal for other models.